

# Chiral condensate in the deconfined phase of quenched gauge theories

Robert G. Edwards

*SCRI, Florida State University, Tallahassee, Florida 32306-4130  
and Jefferson Lab, 12000 Jefferson Avenue, MS 12H2, Newport News, Virginia 23606*

Urs M. Heller

*SCRI, Florida State University, Tallahassee, Florida 32306-4130*

Joe Kiskis

*Department of Physics, University of California, Davis, California 95616*

Rajamani Narayanan

*American Physical Society, One Research Road, Ridge, New York 11961*

(Received 3 November 1999; published 6 March 2000)

We compute the low-lying spectrum of the overlap Dirac operator in the deconfined phase of finite-temperature quenched gauge theory. It suggests the existence of a chiral condensate which we confirm with a direct stochastic estimate. We show that the part of the spectrum responsible for the chiral condensate can be understood as arising from a dilute gas of instantons and anti-instantons.

PACS number(s): 11.15.Ha, 11.30.Rd, 12.38.Gc

## I. INTRODUCTION

The fermion spectrum near zero eigenvalue is closely related to gauge field topology and to chiral symmetry breaking. While there is considerable experimental and theoretical support for chiral symmetry breaking in gauge theories with dynamical quarks at zero temperature and theoretical arguments for its restoration above a critical temperature, the situation is less clear for the nominally simpler case of fermions in the background of quenched gauge fields. To improve our understanding of the quenched, deconfined phase, we have studied the spectrum of the Hermitian overlap Dirac operator [1] in that region. We find a segment of the spectrum concentrated at and near zero eigenvalue and separated from the bulk of the spectrum. The bulk of the spectrum begins to rise rapidly at larger eigenvalues. The exactly zero eigenvalues are associated with the global topology of the gauge field configurations. The statistical properties of the small eigenvalues are in correspondence with predictions from a dilute gas of instantons and anti-instantons. Small, nonzero eigenvalues with these properties give rise to a finite chiral condensate.

Gauge field topology plays a central role in QCD. The presence of gauge field configurations with nontrivial topology indicates that massless fermions will have exact zero modes. These zero modes cause an explicit breaking of the axial U(1) symmetry and result in a massive  $\eta'$  [2]. Conventional wisdom says that the axial U(1) symmetry remains broken at all temperatures since one does not expect a complete suppression of nontrivial gauge field backgrounds. Recent studies using dynamical staggered fermions indicate that the axial symmetry most likely remains broken at high temperatures although the magnitude might be considerably smaller than at low temperatures [3–5]. Since topology is also expected to be suppressed at high temperatures [6], this result is consistent with expectations. Chiral symmetry

breaking, on the other hand, comes from the finite density of eigenvalues near zero [7], so we expect this density to be zero at high temperature in full QCD since chiral symmetry is restored in that case.

The most likely scenario for the spectrum of the massless Dirac operator at high temperatures is to have a delta function at zero due to topology, followed by a gap and a continuous spectrum of eigenvalues resulting in a theory with unbroken chiral symmetry and a broken axial U(1) symmetry. If we adopt the instanton picture for topology, we expect a dilute gas of instantons and anti-instantons at high temperature since the topological susceptibility is highly suppressed. However, this dilute gas of instantons and anti-instantons should not give rise to a chiral condensate in high-temperature, full QCD. A natural explanation in the context of instanton models is that instantons and anti-instantons form molecules at high temperatures [8]. One expects that this formation of molecules is primarily due to interactions induced by fermions [8,9].

In this paper, we will study the spectrum of the massless overlap Dirac operator [1] on the lattice in pure SU(2) and SU(3) gauge theories on lattices with  $N_f=4$  in the deconfined phase. We will study several different ensembles to understand the finite volume effects and also the effect of going deeper into the deconfined phase. In addition to directly studying the spectrum, we will also study the chiral condensate and scalar susceptibility. In some ensembles, we will also compare our results with those obtained using staggered fermions under these conditions.

We have the following results:

(i) The overlap Dirac operator has exact zero eigenvalues indicating that gauge field configurations with nontrivial topology persist in the high temperature phase.

(ii) The spectrum of the nonzero eigenvalues of the overlap Dirac operator has two parts separated by a region in eigenvalue where the density is essentially zero.

(a) The distribution of very small nonzero eigenvalues of the overlap Dirac operator is well-described by a dilute gas of noninteracting instantons and anti-instantons.

(b) The bulk part of the spectrum begins at larger eigenvalue and rises smoothly and steeply.

(iii) The very small eigenvalues of the overlap Dirac operator have the properties that are needed to give a chiral condensate. The separation between the very small eigenvalues and the bulk of the spectrum results in a minimum in the scalar susceptibility.

These features are qualitatively different from the staggered Dirac operator in a quenched theory. The staggered Dirac operator does not have any exact zero eigenvalues. Studies with dynamical staggered fermions have indicated that chiral symmetry is restored at high enough temperatures in QCD with  $N_f$  flavors of massless quarks and also in the quenched theory. Early numerical studies of chiral symmetry restoration at high temperatures using staggered fermions in the “quenched” approximation can be found in Ref. [10]. Further studies using dynamical staggered fermions have established a phase transition showing chiral symmetry restoration at high temperatures. Recent reviews of the lattice results can be found in Ref. [11], and Ref. [12] contains the most recent results for the  $N_T=4$  phase transition.

The lack of exact zero eigenvalues in the staggered fermion spectrum follows from the breaking of the continuum chiral and flavor symmetry at finite lattice spacing [13]. The observed restoration of chiral symmetry at high temperature is consistent with the prediction of Ref. [14] for SU(2) gauge theory with staggered fermions. However, a gap in the spectrum of the staggered Dirac operator at high temperature has not been convincingly established (see, e.g., Ref. [5]). A tail of small eigenvalues seems to persist, possibly consisting of the “shifted” would-be zero modes due to global topology.

The proof of chiral symmetry restoration at high temperature in Ref. [14] is for dynamical fermions, while we are only studying the quenched theory here. So, we could explain the presence, and even accumulation, of very small eigenvalues in the spectrum of the overlap Dirac operator as a quenched artifact. This is not satisfactory, however, since staggered fermions in a quenched theory show no such accumulation of small eigenvalues, but rather a tapering tail of small eigenvalues, indicative of a chirally symmetric phase. As is well known, massless fermions are nontrivial to construct on the lattice [15]. The overlap Dirac operator is one solution to the problem. It is not ultralocal, i.e., its interaction size is not finite, but its interactions are exponentially decreasing with distance. It therefore does not fit into the assumptions used in Ref. [14], and the proof presented there need not hold even in the dynamical theory with overlap fermions. We do not address the issue of the existence of a chirally symmetric phase in the dynamical theory with overlap Dirac fermions in this paper.

Care has to be taken in a finite temperature study in the quenched approximation. In the pure gauge case, gauge field configurations with the Polyakov loop phase near any  $Z_N$  phase are equivalent, related by a global  $Z_N$  symmetry. However, the coupling to fermions is not  $Z_N$  symmetric and the phase with the Polyakov loop along the positive real axis is

preferred. Configurations with “nontrivial expectation value” for Polyakov loop phase can give an “unphysical” signal for a chiral condensate [3] (negative for SU(2) and complex for SU(3) with anti-periodic boundary conditions in the time direction for fermions). In pure SU( $N$ ) gauge theories, configurations with expectation values for the Polyakov lines related by a simple  $Z_N$  factor are equally likely. We will therefore generate pure gauge ensembles so that every configuration has a positive expectation value for the Polyakov loop and impose anti-periodic boundary conditions in the time direction for fermions. So in a sense, this is not a strictly quenched calculation, but has included in it by hand one important feature of the theory with dynamical quarks.

The organization of the paper is as follows. In the second section, we will briefly summarize what we need to know about the overlap Dirac operator. We will present our results for the eigenvalue spectrum in Sec. III and focus on the very small eigenvalues of the overlap Dirac operator. We will show that the spectrum of the very small nonzero and exact zero eigenvalues is described quite well by a noninteracting dilute gas of instantons and anti-instantons. We use the word “dilute” to emphasize that topology is highly suppressed and that the spectrum of these very small eigenvalues is separated from the bulk of the spectrum. We will present our data for the chiral condensate and scalar susceptibility and discuss the relationship between the small, nonzero eigenvalues and the chiral condensate in Sec. IV. Our conclusions are in Sec. V.

Similar studies of the fate of chiral symmetry breaking in the deconfined phase of quenched QCD have been done with domain wall fermions by the Columbia group [16] who measured  $\langle \bar{\psi}\psi \rangle$  and found evidence of topology from its increase at small quark mass and by Lagaë and Sinclair [17] who studied low eigenvalues and meson propagators and found evidence of topology from both.

## II. OVERLAP DIRAC OPERATOR

The massive overlap Dirac operator is given by [1,18]

$$D(\mu) = \frac{1}{2} [1 + \mu + (1 - \mu) \gamma_5 \epsilon(H_w)], \quad (1)$$

with  $0 \leq \mu \leq 1$  describing fermions with positive mass all the way from zero to infinity. The Hermitian operator  $H_w$  is just  $\gamma_5 D_w$  where  $D_w$  is the usual Wilson-Dirac operator with a negative mass on the lattice under consideration.

The propagator for external fermions is given by [1,18]

$$\tilde{D}^{-1}(\mu) = (1 - \mu)^{-1} [D^{-1}(\mu) - 1]. \quad (2)$$

In many cases, it is more convenient to use the Hermitian version,  $H_o(\mu) = \gamma_5 D(\mu)$ . It is easy to see that

$$H_o^2(\mu) = (1 - \mu^2) H_o^2(0) + \mu^2; \quad [H_o^2(0), \gamma_5] = 0. \quad (3)$$

Each eigenvalue  $0 < \lambda^2 < 1$  of  $H_o^2(0)$  is doubly degenerate with opposite chirality eigenvectors. In this basis,  $H_o(\mu)$  and  $D(\mu)$  are block diagonal with  $2 \times 2$  blocks, e.g.,  $D(\mu)$ ,

$$\begin{pmatrix} (1-\mu)\lambda^2 + \mu & (1-\mu)\lambda\sqrt{1-\lambda^2} \\ -(1-\mu)\lambda\sqrt{1-\lambda^2} & (1-\mu)\lambda^2 + \mu \end{pmatrix}, \quad (4)$$

where

$$\gamma_5 = \begin{pmatrix} 1 & 0 \\ 0 & -1 \end{pmatrix}. \quad (5)$$

For a gauge field with topological charge  $Q \neq 0$ , there are, in addition,  $|Q|$  exact zero modes with the chirality sign ( $Q$ ) paired with eigenvectors of opposite chirality and an eigenvalue equal to unity. These are also eigenvectors of  $H_o(\mu)$  and  $D(\mu)$ :

$$D(\mu)_{\text{zero sector}}: \begin{pmatrix} \mu & 0 \\ 0 & 1 \end{pmatrix} \text{ or } \begin{pmatrix} 1 & 0 \\ 0 & \mu \end{pmatrix}, \quad (6)$$

depending on the sign of  $Q$ .

In the chiral eigenbasis of  $H_o^2(0)$ , the external propagator takes the block diagonal form with  $2 \times 2$  blocks,

$$\tilde{D}^{-1}(\mu) = \frac{1}{\lambda^2(1-\mu^2) + \mu^2} \begin{pmatrix} \mu(1-\lambda^2) & -\lambda\sqrt{1-\lambda^2} \\ \lambda\sqrt{1-\lambda^2} & \mu(1-\lambda^2) \end{pmatrix}, \quad (7)$$

and in topologically nontrivial background fields, the  $|Q|$  additional blocks are

$$\begin{pmatrix} \frac{1}{\mu} & 0 \\ \mu & 0 \end{pmatrix} \text{ or } \begin{pmatrix} 0 & 0 \\ 0 & \frac{1}{\mu} \end{pmatrix}, \quad (8)$$

depending on the sign of  $Q$ .

The nontopological contribution to the fermion bilinear, which is the part that will survive the infinite volume limit, is

$$\langle \bar{\psi}\psi \rangle = \left\langle \frac{1}{V} \sum_{\lambda \geq 0} \frac{2\mu(1-\lambda^2)}{\lambda^2(1-\mu^2) + \mu^2} \right\rangle. \quad (9)$$

The chiral condensate is dominated by the small, nonzero eigenvalues. In the thermodynamic limit, it is given by the density of eigenvalues at zero  $\rho(0^+)$ .

A physical quantity that is more sensitive at small quark masses than the chiral condensate is the connected part of the scalar susceptibility. The nontopological contribution to this quantity is

$$\begin{aligned} \chi_{a_0} &= -\frac{1}{V} \langle \text{Tr } \tilde{D}^{-2} \rangle = \left\langle \frac{d}{d\mu} \langle \bar{\psi}\psi \rangle_A \right\rangle \\ &= \left\langle \frac{1}{V} \sum_{\lambda \geq 0} \frac{2(1-\lambda^2)[\lambda^2(1+\mu^2) - \mu^2]}{[\lambda^2(1-\mu^2) + \mu^2]^2} \right\rangle. \end{aligned} \quad (10)$$

This quantity is particularly sensitive to the  $\mu$  dependence of the cancellations between the  $\lambda^2$  and  $\mu^2$  terms in the second factor of the numerator.

TABLE I. Pure gauge ensembles studied. All ensembles have an extent of  $N_T=4$  in the short direction. The number of configurations, the linear extent in the spatial directions, and the estimated temperature are also given.

Gauge group	$\beta$	$N$	$T/T_c$	$L$
SU(2)	2.3	50	1.0	8
SU(2)	2.4	100	1.4	8
SU(2)	2.4	200	1.4	16
SU(2)	2.5	200	2.0	16
SU(3)	5.71	200	1.03	16
SU(3)	5.75	400	1.13	8
SU(3)	5.75	200	1.13	12
SU(3)	5.75	400	1.13	16
SU(3)	5.85	400	1.38	8
SU(3)	5.85	206	1.38	16

Since chiral symmetry is exact on the lattice for the overlap Dirac operator, the pion susceptibility is  $\chi_\pi = (1/\mu) \langle \bar{\psi}\psi \rangle$  [18], and we can define a quantity

$$\begin{aligned} \omega &= \chi_\pi - \chi_{a_0} = \frac{1}{\mu} \langle \bar{\psi}\psi \rangle - \left\langle \frac{d}{d\mu} \langle \bar{\psi}\psi \rangle_A \right\rangle \\ &= \frac{4}{V} \left\langle \sum_{\lambda \geq 0} \frac{\mu^2(1-\lambda_i^2)^2}{[\lambda_i^2(1-\mu^2) + \mu^2]^2} \right\rangle. \end{aligned} \quad (11)$$

This is a measure of the  $U(1)_A$  symmetry breaking in a dynamical theory. It is strictly positive and is not sensitive to cancellations like those within the sum for  $\chi_{a_0}$  in Eq. (10). Due to the higher powers of the quark mass and eigenvalues in the sum, it is more sensitive than the chiral condensate to small eigenvalues.

### III. EIGENVALUE SPECTRUM

We will investigate the quark spectrum on the ensembles of pure SU(2) and SU(3) gauge theory configurations listed in Table I. At  $N_T=4$ , the critical coupling is  $\beta_c = 2.2986(6)$  for SU(2) and  $\beta_c = 5.6925(2)$  for SU(3) [19]. All ensembles in Table I are in the deconfined phase.

The low-lying eigenvalues of  $H_0^2$  (including the exact zero modes) and  $D_s D_s^\dagger$  ( $D_s$  is the massless staggered operator) were computed using the Ritz variational technique [20]. In order to deal numerically with the overlap Dirac operator, it is necessary to use a representation for  $\epsilon(H_w)$ , and we used the optimal rational approximation [21]. We compare the low lying spectrum of the staggered and overlap Dirac operator for two typical ensembles, SU(2) at  $\beta=2.4$  and SU(3) at  $\beta=5.75$ , both on  $16^3 \times 4$  lattices, in Fig. 1. We see a remarkable difference. Both staggered and overlap spectrum show a rapidly rising bulk. But while the staggered spectrum has a rapidly decreasing tail of small eigenvalues, the overlap spectrum shows an accumulation of very small, but non-zero, eigenvalues.

The spectral distributions of the overlap Dirac operator

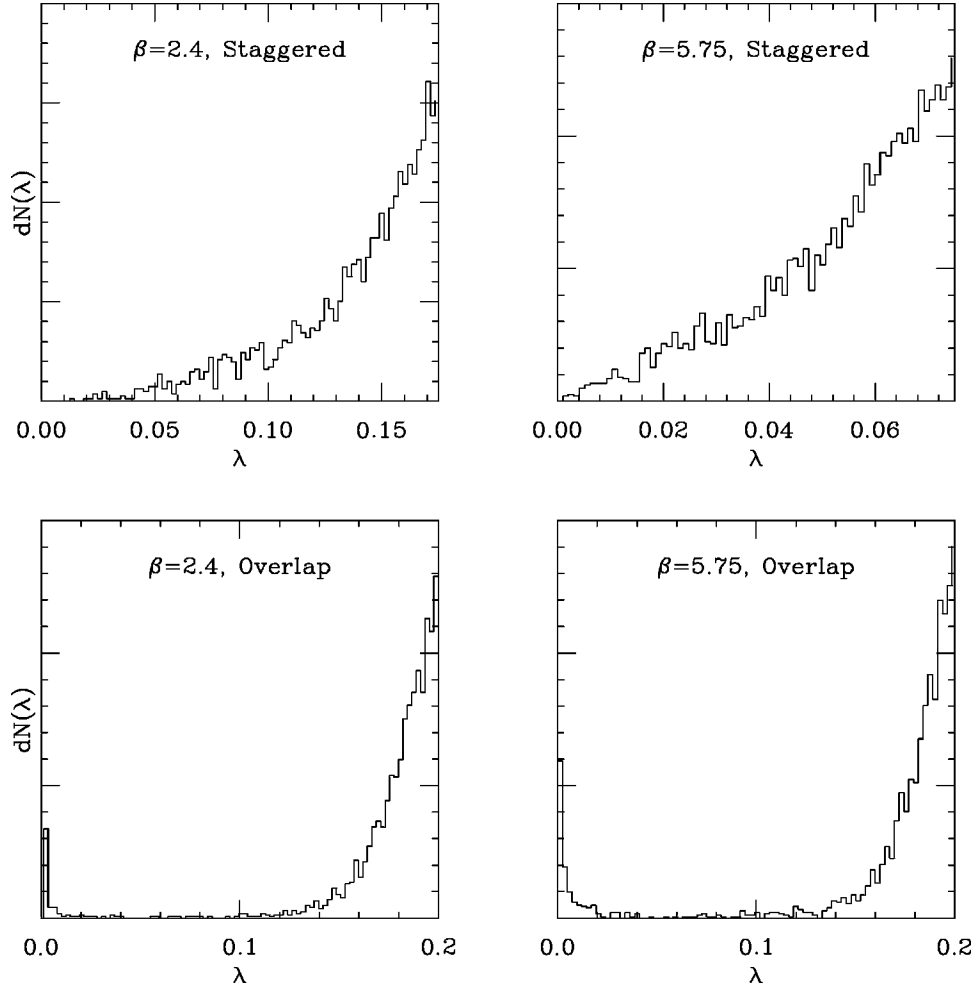


FIG. 1. Histogram of the low-lying eigenvalues of the staggered and overlap Dirac operator for the SU(2) ensemble at  $\beta=2.4$  and the SU(3) ensemble at  $\beta=5.75$ . Both lattices have a spatial volume of  $16^3$ . For the overlap Dirac operator the exact zero modes are not shown.

for all the ensembles in Table I have the same qualitative features:

(i) There is a typical scale ( $\lambda=0.05$ ) independent of the ensemble that separates the spectrum into two parts: “small” ( $<0.05$ ) and “large” ( $>0.05$ ) eigenvalues.<sup>1</sup>

(ii) Small eigenvalues occur in all topological sectors.

(iii) The number of small eigenvalues per unit of lattice volume remains roughly constant at fixed coupling under changes of the volume and decreases as one goes deeper into the deconfined phase.

In this section, we focus on the statistical properties of the low-lying eigenvalues of the overlap Dirac operator. Our conclusion is that it is roughly consistent with the data to associate each nonzero pair of small eigenvalues with an instanton and/or anti-instanton pair. Topics related to the magnitude of the eigenvalues are discussed in the next section.

<sup>1</sup>We note here that the smallest eigenvalue for the free overlap Dirac operator with anti-periodic boundary conditions in the temperature direction is 0.238 and 0.200 for a Wilson mass of 1.5 and 1.8, respectively, at  $N_T=4$ .

We approach the hypothesis in steps of increasing specificity. Let  $n_+$  and  $n_-$  be the number of separated, localized instantons and anti-instantons, respectively. Then the topological charge of the configuration, as determined by the fermions, is  $Q=n_+-n_-$  and the total number of objects is  $n \equiv n_++n_-$ .

For infinite separation between instantons and anti-instantons, this gives  $n$  zero eigenvalues. At large but finite separation, we expect  $|Q|$  exactly zero eigenvalues and  $n-|Q|=2 \min(n_+, n_-)$  small eigenvalues. Since the nonzero eigenvalues come in  $\pm\lambda$  pairs, we associate each nonzero pair of small eigenvalues with an instanton and/or anti-instanton pair. The number of exact zero modes of  $H_0^2$  in a fixed gauge field background is equal to the net number of levels crossing zero in the spectral flow of  $H_w$  [22]. In addition, individual levels crossing zero in the spectral flow of  $H_w$  can be associated with instantons in the background gauge field [23,24]. We performed a spectral flow on several of the ensembles in Table I and found that there is essentially a one-to-one agreement: If  $n_+$  ( $n_-$ ) levels crossed zero from above (below), then there were  $n-|Q|=2 \min(n_+, n_-)$  small eigenvalues for the overlap Dirac operator in addition to the rigorously expected  $|Q|=|n_+-n_-|$ .

TABLE II. Distribution of the number of topological objects along with predictions from a Poisson distribution.

	SU(2)	SU(2)	SU(2)	SU(2)	SU(3)	SU(3)	SU(3)	SU(3)	SU(3)	SU(3)
$\beta$	2.3	2.4	2.4	2.5	5.71	5.75	5.75	5.75	5.85	5.85
$L$	8	8	16	16	16	8	12	16	8	16
$N$	50	100	200	200	200	400	200	400	400	206
$n=0$	11(10)	74(75)	27(28)	130(130)	1(1)	286(290)	83(77)	38(35)	379(378)	144(137)
$n=1$	13(16)	23(22)	57(55)	57(56)	5(6)	100(93)	63(73)	76(85)	19(22)	43(56)
$n=2$	14(13)	3(3)	58(54)	10(12)	8(16)	13(15)	39(35)	105(104)	2(1)	17(11)
$n=3$	8(7)		32(35)	3(2)	28(27)	1(2)	11(11)	95(84)		1(2)
$n=4$	2(3)		16(17)		46(35)		3(3)	46(51)		1(0)
$n=5$	2(1)		4(7)		38(35)		1(1)	25(25)		
$n=6$			3(2)		34(30)			9(10)		
$n=7$			3(1)		17(21)			5(4)		
$n=8$					10(14)			1(1)		
$n=9$					6(8)					
$n=10$					2(4)					
$n=11$					3(2)					
$n=12$					2(1)					
$\langle n \rangle / V$	1.66	0.29	0.25	0.05	0.63	0.32	0.28	0.31	0.06	0.05
Ratio	0.97	1.09	0.93	0.99	1.15	1.08	0.92	1.02	0.90	0.83

$-n_-$  exact zero eigenvalues. Therefore our association of small eigenvalues of  $H_0$  with instanton and/or anti-instanton pairs is well justified.

For finite temperature with  $T > T_c$ , the distribution of instanton sizes increases steeply with instanton size until it is cut off on the large size end by  $N_T$ . Thus most of the instantons have a size not too far from  $N_T$ . We will always use a simple model in which the instantons and anti-instantons are assumed to be at a sufficiently large separation that their interactions due to the pure gauge action can be neglected.

With the assumption that the  $n$  objects are noninteracting, the number per configuration should have a Poisson distribution

$$P(n, \langle n \rangle) = \langle n \rangle^n e^{-\langle n \rangle} / n!, \quad (12)$$

where  $\langle n \rangle$  is the average of the distribution. For a Poisson distribution, the average and variance are equal. We present our data for the distribution of  $n$  as counted by the fermions in Table II. The average of the distribution per  $8^3$  lattice volume is shown in the same table. The numbers in parentheses are the predictions of the distribution using the average value in Eq. (12). We also write down the ratio of the variance and the average in the table. The data are in fairly good agreement with the Poisson distribution.

To the extent that the  $n$  zero and small eigenvalues can be associated with any sort of objects localized in three space or Euclidean four space, the number of objects and  $n$  should, at fixed  $N_T$  and fixed coupling  $g^2$ , be proportional to the spatial volume  $V$  in lattice units. This is roughly supported by the SU(2) and SU(3) data in Table II. If the localized objects are instantons, then we also expect the density to decrease rapidly with decreasing  $g^2$ . This is also seen in the data.

At the next level of detail, we can distinguish between the contributions to  $n$  from  $n_+$  and  $n_-$ . If the instantons and anti-instantons are thrown into the configurations independently (without interaction), then for a fixed  $n$  the relative probabilities in the  $(n_-, n_+)$  distribution will be given by the binomial coefficients

$$B(n_+, n_- | n) = \frac{1}{2^n} \frac{n!}{n_+! n_-!}. \quad (13)$$

Combining this with  $\langle n \rangle$  values from the data gives predictions for the numbers  $n_+$  and  $n_-$  of positive and negative chirality states. We combine  $(n_+, n_-)$  with  $(n_-, n_+)$  and compare the data and predictions in Table III. In almost all of the cases, the difference is within the statistical error expected from the value of the predicted number.

Finally, the assumption of a noninteracting gas of instantons and anti-instantons leads to a simple expression for the distribution of topological charge,

$$T(Q) = e^{-\langle n \rangle} I_Q(\langle n \rangle), \quad (14)$$

where  $I_Q$  is the modified Bessel function of order  $Q$ . Our data can be cross-checked against this prediction also, and this is shown in Table IV. Again, we see fairly good agreement with the data. We also note that  $\langle Q^2 \rangle = \langle n \rangle$  under this assumption, and this is essentially the case when we compare Table II and Table IV.

This simple model of associating the zero and the small, nonzero eigenvalues with independent instantons and anti-instantons seems to account for the main statistical properties of the  $n_+, n_-$  data.



TABLE III. Distribution of the number of instantons for a fixed number of topological objects (less than eight) along with predictions from binomial distribution using the Poisson average.

	SU(2)	SU(2)	SU(2)	SU(2)	SU(3)	SU(3)	SU(3)	SU(3)	SU(3)	SU(3)
$\beta$	2.3	2.4	2.4	2.5	5.71	5.75	5.75	5.75	5.85	5.85
$L$	8	8	16	16	16	8	12	16	8	16
$N$	50	200	200	200	200	400	200	400	400	206
$n=2, n_+=0$	6(7)	2(2)	33(27)	6(6)	1(8)	6(8)	20(18)	54(52)	2(0)	8(6)
$n=2, n_+=1$	8(7)	1(2)	25(27)	4(6)	7(8)	7(8)	19(18)	51(52)	0(0)	9(6)
$n=3, n_+=0$	1(2)		12(9)	0(0)	7(7)	0(0)	3(3)	25(21)		0(0)
$n=3, n_+=1$	7(5)		20(27)	3(1)	21(21)	1(1)	8(8)	70(63)		1(1)
$n=4, n_+=0$	1(0)		2(2)		9(4)		0(0)	9(6)		0(0)
$n=4, n_+=1$	1(2)		6(9)		18(17)		2(1)	30(26)		1(0)
$n=4, n_+=2$	0(1)		8(6)		19(13)		1(1)	7(19)		0(0)
$n=5, n_+=0$	0(0)		0(0)		1(2)		0(0)	2(2)		
$n=5, n_+=1$	1(0)		1(2)		10(11)		0(0)	9(8)		
$n=5, n_+=2$	1(1)		3(4)		27(22)		1(0)	14(16)		
$n=6, n_+=0$			0(0)		1(1)			0(0)		
$n=6, n_+=1$			0(0)		7(6)			3(2)		
$n=6, n_+=2$			2(1)		19(14)			2(5)		
$n=6, n_+=3$			1(1)		7(9)			4(3)		
$n=7, n_+=0$			0(0)		1(0)			0(0)		
$n=7, n_+=1$			0(0)		1(2)			0(0)		
$n=7, n_+=2$			1(0)		3(7)			1(1)		
$n=7, n_+=3$			2(0)		12(12)			4(2)		

TABLE IV. Distribution of topological charge along with the prediction based on a noninteracting gas of instantons and anti-instantons using the average from the Poisson distribution.

	SU(2)	SU(2)	SU(2)	SU(2)	SU(3)	SU(3)	SU(3)	SU(3)	SU(3)	SU(3)
$\beta$	2.3	2.4	2.4	2.5	5.71	5.75	5.75	5.75	5.85	5.85
$L$	8	8	16	16	16	8	12	16	8	16
$N$	50	200	200	200	200	400	200	400	400	206
$Q=0$	19(17)	75(76)	61(62)	134(136)	38(36)	293(297)	103(96)	101(110)	379(378)	153(143)
$Q=1$	21(22)	23(22)	82(86)	60(57)	67(65)	101(95)	72(82)	164(166)	19(22)	44(57)
$Q=2$	7(8)	2(2)	41(37)	6(6)	45(47)	6(8)	22(19)	86(83)	2(0)	9(6)
$Q=3$	2(2)		14(11)		26(28)		3(3)	35(30)		
$Q=4$	1(0)		2(3)		18(14)			12(9)		
$Q=5$					3(6)			2(2)		
$Q=6$					1(2)					
$Q=7$					1(1)					
$Q=8$										
$Q=9$										
$Q=10$					1(0)					
$\langle Q^2 \rangle / V$	1.66	0.31	0.25	0.05	0.64	0.31	0.28	0.33	0.07	0.05

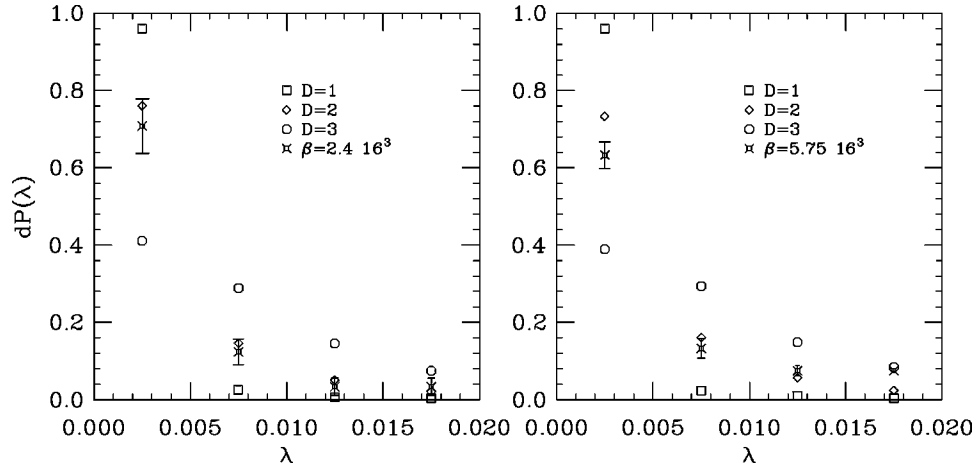


FIG. 2. Histogram of the small eigenvalues along with the histogram from the toy model for  $D=1,2,3$  with the appropriate value of  $\langle n \rangle$  from Table II for the SU(2) ensemble at  $\beta=2.4$  and the SU(3) ensemble at  $\beta=5.75$ . Both lattices have a spatial volume of  $16^3$ .

#### IV. SMALL EIGENVALUES AND A CHIRAL CONDENSATE

This section deals with the spectrum of the small, nonzero eigenvalues. We begin with a discussion relating the spectrum to expectations from the instanton–anti-instanton gas model. This is followed by an analysis of the way in which these eigenvalues contribute to physical quantities such as the chiral condensate.

In the previous section, we were only concerned with the number of small eigenvalues (eigenvalues below 0.05) in each configuration. Our computation of the low-lying eigenvalues of  $H_o^2$  along with the spectral flow of  $H_w$  enables us to obtain this number with very good certainty per configuration. Because of the numerical accuracies involved, the small eigenvalues can be trusted only with an absolute accuracy of 0.005, and we can create a histogram of the low-lying eigenvalues with a bin width of 0.005 giving us a total of ten bins in each ensemble.

A detailed analysis of the relationship of small eigenvalues, instantons, and the condensate at zero temperature can be found in [25]. It was shown there that the spectrum from a model with fermions in a background of dilute instantons and anti-instantons gives a chiral condensate and is consistent with chiral random matrix theory. Some discussion of the finite temperature spectrum appears in [8]. We have used a much simpler version of these ideas.

The most important effect for widely separated instantons and anti-instantons is from the mixing of the  $n$  would-be zero modes of the fermions. At infinite separation, there would be  $n$  modes with  $\lambda=0$ . At finite temperature and in the continuum, the spatial tails of these wave functions are exponential. Further, a configuration with, e.g.,  $n=n_+$  has that number of exact zero modes. This leads us to a model with instantons and anti-instantons that are still distributed independently over the configurations and with an  $n \times n$  interaction matrix for the  $n$  modes that is made up of  $n_+ \times n_+$  and  $n_- \times n_-$  blocks on the diagonal and  $n_- \times n_+$  and  $n_+ \times n_-$  off-diagonal blocks. The diagonal blocks corresponding to instanton–instanton fermion mode interactions and to anti-

instanton–anti-instanton fermion mode interactions, including self-interactions, are zero.

$$T_{ij}=0 \quad \text{if } i \text{ and } j \text{ are both instantons}$$

$$\text{or both anti-instantons.} \quad (15)$$

In the off-diagonal blocks there is an entry for each ordered way that an instanton can be paired with an anti-instanton. It has the form

$$T_{ij}=h_0 e^{-d(i,j)/D} \quad \text{if } (i,j) \text{ is an instanton–anti-instanton pair} \quad (16)$$

The energy scale is determined by the constant  $h_0$ . The distance between the instanton and/or anti-instanton pair is  $d(i,j)$ . The length scale of the mode interactions is  $D$ . We expect  $D$  to be of order  $N_T$  since that is the range of the continuum mode tails.

The next step is to generate data from the model and compare it with the real data. The model calculation is in the continuum with periodic boundary conditions, so that  $d(i,j)$  is the shortest distance connecting the pair. The  $(n_+, n_-)$  values are distributed according to Eq. (12) and Eq. (13) with  $\langle n \rangle$  obtained from Table II. The positions of the instantons and anti-instantons are selected at random. Then the matrix elements of  $T$  are computed. Finally the eigenvalues of  $T$  are computed. Note that for a matrix with the form of  $T$ , the spectrum has  $|Q|$  zeros and  $(n - |Q|)/2$  pairs  $\pm \lambda$ . This process is repeated for many configurations. The resulting set of eigenvalue distributions is then compared with the data from the various ensembles. The conclusion is that a value of  $D=2$  best fits the data for all the ensembles. We have shown the comparison between the real data and the toy model for two of the cases in Fig. 2. Thus the spectrum of the small eigenvalues can also be explained by the simple instanton–anti-instanton gas picture.

A physical role for these modes is suggested by the fact that the chiral condensate is determined by the infinite-volume fermion spectral density at zero eigenvalue. The most straightforward thing to do would be to use the com-

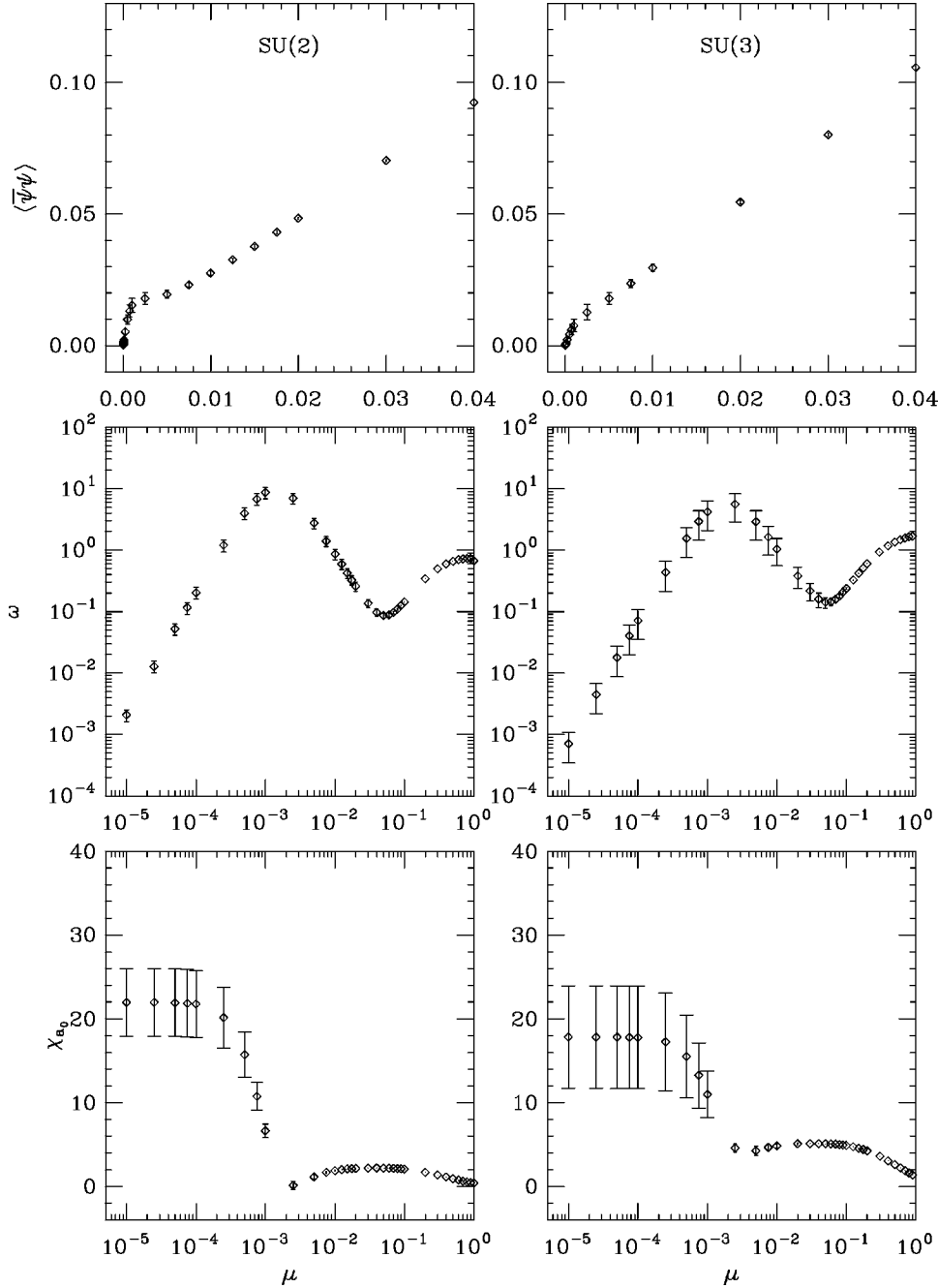


FIG. 3. The stochastic estimates of  $\langle \bar{\psi}\psi \rangle$ ,  $\omega$  and  $\chi_{a_0}$  for the SU(2) ensemble at  $\beta=2.4$  and SU(3) ensemble at  $\beta=5.75$ . Both lattices have a spatial volume of  $16^3$ .

puted eigenvalues to do the sums in Eqs. (9)–(11) for the condensate,  $\omega$ , and  $\chi_{a_0}$ . However, we need the  $\mu \rightarrow 0$  limit, and it is apparent from the forms of the sums that they are very sensitive to the positions of the eigenvalues when  $\mu$  is very small. As mentioned earlier in this section, the small eigenvalues are not precisely known, so that the value of the sum is unreliable for  $\mu$  less than about 0.01, and this is not small enough to be useful.

However, it is possible to compute the chiral condensate,  $\omega$ , and  $\chi_{a_0}$  by a stochastic method using the overlap Dirac

operator. The method is specific to the overlap Dirac operator and is described in Refs. [18,24]. Using this method, we have computed the condensate, the anomalous  $U(1)_A$  breaking, and the scalar susceptibility for the SU(2) ensemble with  $\beta=2.4$  on the  $16^3$  lattice and for the SU(3) ensemble with  $\beta=5.75$  also on the  $16^3$  lattice. The results are shown in Fig. 3. If the steep decrease of the condensate toward zero below  $\mu=0.002$  is interpreted as a finite volume effect, then these data are evidence for chiral symmetry breaking. Additional evidence for chiral symmetry breaking can be seen in the



plots for  $\omega$ . We see there is a quark mass region in the nontopological contribution to  $\omega$  from  $\mu=0.002$  to 0.05 where the expected divergence of  $1/\mu$  sets in. The region below  $\mu=0.002$  is where the finite volume effects become large.

The shapes of the curves in Fig. 3 are consistent with the qualitative features of the computed eigenvalues; small eigenvalues concentrated close to  $\lambda=0$ , a sparsely populated region around  $\lambda=0.05$ , and the dense eigenvalues of the bulk of the spectrum beginning at a larger eigenvalue. The strongest effect is a dip in  $\chi_{a_0}$  due to the presence of two terms in the sum in Eq. (10) with opposite signs, along with a spectral distribution that has two regions (a small eigenvalues region and a bulk region) separated by a sparsely populated region around  $\lambda=0.05$  as seen in Fig. 1.

One may ask whether the simple model, which reproduces the properties of the small eigenvalues, gives a chiral condensate. The short answer to that question is yes. Our model is just a simplification of the model in Ref. [25], which does give a condensate. The longer answer comes after testing the simplified model itself for the necessary properties. With  $\langle n \rangle/V$  fixed and increasing  $V$ , the staircase function

$$N(\lambda, V) = \int_0^\lambda d\sigma \rho(\sigma, V) \quad (17)$$

in the large  $V$  and small  $\lambda$  region needs to approach a function of  $\lambda V$  that is linear for large  $\lambda V$ .  $N(\lambda, V)$ , as computed with modest statistics from the model eigenvalues, is consistent with that behavior. Thus it appears that the eigenvalues in the small region of the spectrum are sufficient to give rise to a condensate.

## V. CONCLUSIONS

We have studied the spectrum of the overlap Dirac operator on several quenched ensembles in the deconfined phase. We find clear evidence for topology in the deconfined phase. We also found that the topological susceptibility decreases sharply as we go deeper into the deconfined phase. The gauge field contains instanton and anti-instanton-like objects which are well-described as a dilute gas. This is supported by a part of the spectrum of the overlap Dirac operator consisting of small (in our case  $<0.05$ ) eigenvalues which are well separated from the bulk. This small part is consistently described as arising from a dilute gas of instantons and anti-instantons. It appears that the small eigenvalues produced by such a dilute gas are sufficient to create a chiral condensate and hence spontaneous chiral symmetry breaking even in the deconfined phase of quenched gauge theories.

## ACKNOWLEDGMENTS

We would like to thank the Aspen Center for Physics where part of this work was carried out. We would also like to thank Herbert Neuberger, Philippe de Forcrand, and Poul Damgaard for discussions. U.M.H. and R.G.E. were supported in part by DOE contracts DE-FG05-85ER250000 and DE-FG05-96ER40979. R.G.E. was also supported by DOE contract DE-AC05-84ER40150 under which the Southeastern Universities Research Association (SURA) operates the Thomas Jefferson National Accelerator Facility. Computations were performed on the CM-2, QCDSF, and workstation clusters at SCRI and the University of California at Davis.

- 
- [1] H. Neuberger, Phys. Lett. B **417**, 141 (1998).
  - [2] G. 't Hooft, Phys. Rev. Lett. **37**, 8 (1976); Phys. Rev. D **14**, 3432 (1976).
  - [3] S. Chandrasekharan, D. Chen, N. Christ, W. Lee, R. Mawhinney, and P. Vranas, Phys. Rev. Lett. **82**, 2463 (1999).
  - [4] C. Bernard *et al.*, Phys. Rev. Lett. **78**, 598 (1997).
  - [5] J.B. Kogut, J.-F. Lagaë, and D.K. Sinclair, Phys. Rev. D **58**, 054504 (1998).
  - [6] M. Müller-Preussker, in *Proceedings of the XXVI International Conference on High Energy Physics*, edited by James R. Stanford (American Institute of Physics, New York, 1992), Vol. 2, p. 1545; S. Gottlieb *et al.*, Phys. Rev. D **47**, 3619 (1993).
  - [7] T. Banks and A. Casher, Nucl. Phys. **B169**, 125 (1980).
  - [8] T. Schäfer, E.V. Shuryak, and J.J.M. Verbaarschot, Phys. Rev. D **51**, 1267 (1995).
  - [9] E.-M. Ilgenfritz and E.V. Shuryak, Phys. Lett. B **325**, 263 (1994); T. Schäfer and E.V. Shuryak, Phys. Rev. D **53**, 6522 (1996).
  - [10] J. Kogut, H. Matsuoka, M. Stone, H.W. Wyld, S. Shenker, J. Shigemitsu, and D.K. Sinclair, Nucl. Phys. **B225**, 93 (1983); Phys. Rev. Lett. **51**, 869 (1983).
  - [11] A. Ukawa, Nucl. Phys. B (Proc. Suppl.) **53**, 106 (1997); E. Laermann, *ibid.* **63**, 114 (1998).
  - [12] C. Bernard, C. DeTar, S. Gottlieb, U.M. Heller, J. Hetrick, K. Rummukainen, R.L. Sugar, and D. Toussaint, Phys. Rev. D **61**, 054503 (2000).
  - [13] J.C. Vink, Phys. Lett. B **210**, 211 (1998).
  - [14] E.T. Tomboulis and L.G. Yaffe, Phys. Rev. Lett. **52**, 2115 (1984).
  - [15] H.B. Nielsen and M. Ninomiya, Nucl. Phys. **B185**, 20 (1981); **B193**, 173 (1981); Phys. Lett. **105B**, 219 (1981).
  - [16] P. Chen *et al.*, Nucl. Phys. B (Proc. Suppl.) **73**, 207 (1999); High Energy Physics, Vancouver (1998), Vol. 2, p. 1802 (hep-lat/9812011).
  - [17] J.-F. Lagaë and D.K. Sinclair, hep-lat/9909097.
  - [18] R.G. Edwards, U.M. Heller, and R. Narayanan, Phys. Rev. D **59**, 094510 (1999).
  - [19] J. Fingberg, U.M. Heller, and F. Karsch, Nucl. Phys. **B392**, 493 (1993).
  - [20] B. Bunk, K. Jansen, M. Lüscher, and H. Simma, DESY Report, 1994; T. Kalkreuter and H. Simma, Comput. Phys. Commun. **93**, 33 (1996).
  - [21] R.G. Edwards, U.M. Heller, and R. Narayanan, Nucl. Phys. **B540**, 457 (1999); Parallel Comput. **25**, 1395 (1999).

- [22] R. Narayanan and H. Neuberger, Phys. Rev. Lett. **71**, 3251 (1993); Nucl. Phys. **B412**, 574 (1994).
- [23] R.G. Edwards, U.M. Heller, and R. Narayanan, Phys. Rev. D **60**, 034502 (1999).
- [24] R.G. Edwards, U.M. Heller, and R. Narayanan, Nucl. Phys. **B535**, 403 (1998).
- [25] J. Verbaarschot, Nucl. Phys. **B427**, 534 (1994); D. Dyakonov and V. Petrov, Phys. Lett. **147B**, 351 (1984); E. Shuryak and J. Verbaarschot, Nucl. Phys. **B341**, 1 (1990).